# Design and Characterization of Chemically Stabilized Aβ42 Oligomers

**ARTICLE** *in* BIOCHEMISTRY · AUGUST 2015

Impact Factor: 3.02 · DOI: 10.1021/acs.biochem.5b00318 · Source: PubMed



**3 AUTHORS**, INCLUDING:

Ghiam Yamin

University of California, San Diego

**22** PUBLICATIONS **1,245** CITATIONS

SEE PROFILE

David Teplow

University of California, Los Angeles

**245** PUBLICATIONS **26,580** CITATIONS

SEE PROFILE

# Design and characterization of chemically stabilized Aβ42 oligomers



| | |
|---|---|
| Journal: | *Biochemistry* |
| Manuscript ID: | bi-2015-00318s.R2 |
| Manuscript Type: | Article |
| Date Submitted by the Author: | n/a |
| Complete List of Authors: | Yamin, Ghiam; University of California, San Diego, Radiology<br>Huynh, Tien-Phat; Washington University at St. Louis, Neurology<br>Teplow, David; UCLA, Neurology |
| | |

# Design and characterization of chemically stabilized Aβ42 oligomers

Ghiam Yamin[1, 3, †], Tien-Phat Vuong Huynh[2, †], and David B. Teplow[3*]

[1]Department of Radiology, University of California San Diego School of Medicine, San Diego, CA; [2]Department of Neurology, School of Medicine, Washington University at St. Louis, St. Louis, MO; [3]Department of Neurology, David Geffen School of Medicine at UCLA, Los Angeles, CA

[†]These authors contributed equally to the manuscript

*Send all correspondence to dteplow@mednet.ucla.edu

Keywords: Amyloid β-protein (Aβ), PICUP, cross-linking, oligomers

Running Title: Scanning PICUP of Aβ

Funding Sources: We gratefully acknowledge support from the UCLA Medical Scientist Training Program (MSTP) (GY), the UCLA Chemistry-Biology Interface (CBI) Training Program (GY), NIH Grants NS038328 (DBT), AG027818, and AG041295 (DBT), and the Jim Easton Consortium for Drug Discovery and Biomarkers at UCLA (DBT).

## ABSTRACT

A popular working hypothesis of Alzheimer's disease causation is amyloid β-protein oligomers are the key neuropathogenetic agents. To rigorously elucidate the role of oligomers requires the production of stable oligomers of each size. We previously used zero-length photochemical cross-linking to enable stabilization, isolation, and determination of structure–activity relationships of pure populations of Aβ40 dimers, trimers, and tetramers. We also attempted to study Aβ42, but found that Aβ42 oligomers subjected to the same procedures were not completely stable. Based on the fact that Tyr is a critical residue in the cross-linking chemistry, we reasoned that chemical accessibility of Tyr10 in Aβ42 must differ from that in Aβ40. We thus chemically synthesized four singly substituted Tyr variants that placed the Tyr in different positions across the Aβ42 sequence. We then studied the stability of the resulting cross-linked oligomers as well as procedures for fractionating the oligomers to obtain pure populations of different sizes. We found that [Phe$^{10}$, Tyr$^{42}$]Aβ42 produced stable oligomers yielding highly pure populations of dimers through heptamers. This provides the means to establish formal structure-activity relationships of these important Aβ42 assemblies. In addition, we were able to analyze the dissociation patterns of non-cross-linked oligomers to produce a model for oligomer formation. This work is relevant to the determination of structure–activity relationships that have the potential to provide mechanistic insights into disease pathogenesis.

## INTRODUCTION

Alzheimer's disease (AD) is a neurodegenerative disorder that causes irreversible damage to the brain that manifests in memory loss, cognitive dysfunction, and eventual death. AD is characterized by the cerebral deposition of plaques composed of aggregated fibrils of the amyloid β-protein (Aβ), a 40-42 amino acid peptide. These aggregates long were believed to be the proximate neurotoxins in AD. However, this idea has been supplanted by the working hypothesis that Aβ oligomers are more relevant etiologic targets [1-7]. Designing therapeutic agents specific for "oligomers" requires establishing accurate structure-neurotoxicity relationships. Unfortunately, Aβ is an intrinsically disordered protein that self-associates to form oligomers that are metastable and polydisperse—factors that largely have prevented formal structure-neurotoxicity studies.

A fruitful approach for stabilizing oligomers of specific size has been zero-length cross-linking using the technique of Photo-Induced Cross-linking of Unmodified Proteins (PICUP) [8]. Oligomers stabilized in this manner do not self-associate or dissociate [9, 10]. This has allowed the fractionation and purification of stable Aβ40 oligomers of specific size using SDS-PAGE [10]. These cross-linked oligomers demonstrated similar or more robust neurotoxic activity than did non-cross-linked Aβ40 oligomers [10].

To study the more clinically relevant Aβ42 isoform of Aβ, we subjected monomeric Aβ42 to PICUP, SDS-PAGE, and extraction. We were surprised to observe that, unlike cross-linked oligomers of Aβ40, the Aβ42 oligomers were not fully stable and thus exhibited partial dissociation in subsequent SDS gels. The phenolic side-chain of the amino acid Tyr is highly reactive in PICUP chemistry [8]. It can form di-tyrosine and tri-tyrosine bonds among different Aβ monomers, as well as covalent bonds between Tyr

on different closely associated peptide chains and inter- and intra-molecular covalent bonds between Tyr and nucleophilic side chains such as that of lysine [8]. *In vitro* and *in silico* studies have revealed significant differences between Aβ40 and Aβ42 in their conformational dynamics, oligomerization, and fibril formation [9, 11]. Conformational differences within the respective Aβ monomers must account for these observations, a conclusion suggesting that Tyr in Aβ42, relative to Aβ40, may be less chemically accessible, shielded, or located in a structurally labile position, preventing complete cross-linking and predisposing oligomers produced thereof to dissociate. If so, we reasoned that repositioning a Tyr residue at different sites along the peptide chain could provide the means to more efficient cross-linking. We thus chemically synthesized Aβ42 variants with Tyr substituted at four different locations between the N- and C-termini-Asp1, Phe20, Ala30, and Ala42. We report here the results of studies of the stabilities of these peptides and how these stabilities may be used to model the Aβ42 oligomerization process.

## MATERIALS AND METHODS

### *Chemicals and Reagents*

Chemicals were obtained from Sigma-Aldrich and were of the highest purity available. Tris-2,2′-bipyridyl-dichlororuthenium(II) hexahydrate ($Ru(Bpy)_3$), ammonium persulfate (APS), and SimplyBlue™ SafeStain (Coomassie G-250) were purchased from Invitrogen (Carlsbad, CA). Acrylamide and TEMED were purchased from Bio-Rad (Hercules, CA). N, N'-methylene-bis-acrylamide was purchased from Sigma-Aldrich (St. Louis, MO). All solutions were prepared in double-distilled de-ionized (DDI) water produced from a Milli-Q system (Millipore Corp., Bedford, MA).

### *Peptide Design and Synthesis*

Aβ42 peptides were synthesized using 9-fluorenylmethoxycarbonyl (Fmoc) chemistry, purified by reverse phase-high performance liquid chromatography, and characterized by mass spectrometry and amino acid analysis, as described previously [12]. Quantitative amino acid analysis and mass spectrometry yielded the expected compositions and molecular weights, respectively, for each peptide (see Fig. 1 for peptide sequences). $Tyr^{10}$ was replaced by $Phe^{10}$ in each of the four Aβ42 variants. This was done to prevent intramolecular cross-linking and multipoint intermolecular cross-linking, each of which would complicate the analysis of cross-linking patterns. We have shown in prior published work that the Tyr10Phe substitution does not alter the oligomerization process [13]. Purified peptides were stored as lyophilizates at -20°C.

### *Preparation of Aβ Solutions*

Stock solutions of Aβ were prepared by reconstituting lyophilized peptide in a 1:4.5:4.5 (v/v/v) ratio of 60 mM NaOH:Milli-Q water:22.2 mM sodium phosphate, pH 7.5, to yield a nominal Aβ concentration of 1 mg/mL in 10 mM sodium phosphate, pH 7.5. The peptide solution then was sonicated for 1 min in a bath sonicator (Branson Model 1510, Danbury, CT) and filtered through a 30 kDa molecular weight cutoff Microcon centrifugal filter device (Millipore, Billerica, MA) for 15 min at room temperature (RT; 22 °C) at 16,000 × ***g***. The filtrate was collected and the Aβ concentration was determined by UV absorbance ($\varepsilon_{280}$=1280 $cm^{-1}$ $M^{-1}$) using a 1 cm quartz cuvette (Hellma, Plainview, NY) and a Beckman DU-640 spectrophotometer (Beckman Instruments, Fullerton, CA). All measurements were performed at RT. This protocol results in uniform and reproducible material termed low molecular weight (LMW) Aβ [14].

***Cross-linking, SDS-PAGE, and Gel Staining***

Peptides were covalently cross-linked using the technique of Photo-Induced Cross-linking of Unmodified Proteins (PICUP) immediately after LMW preparation [15]. Briefly, 3 μL of 2 mM $Ru(Bpy)_3$ and 3 μL of 40 mM APS were added to 54 μL of 80 μM Aβ42 (or its analogues) in 10 mM sodium phosphate buffer, pH 7.5. The final Aβ:$Ru(Bpy)_3$:APS molar ratios were 0.72:1:20. The mixture was irradiated for 1 s with a with a "Fiber-Lite" high intensity visible light source (Dolan-Jenner, Boxborough, MA) and the reaction was immediately quenched with 1 μL of 1 M dithiothreitol (DTT) in 10 mM sodium phosphate buffer, pH 7.4. For each reaction, APS and $Ru(Bpy)_3$ were added to the Aβ solution and the mixture vortexed for 1 s after addition of the cross-linking reagents and immediately preceding irradiation. Two reactions tubes typically were cross-linked and quenched to produce a total volume of 122 μL.

For SDS-PAGE analysis, the 122 μL of cross-linked Aβ was mixed with 122 μL of 2× Tricine sample buffer (Invitrogen, Carlsbad, CA). Two-hundred μL of this cross-linked oligomer mixture was boiled for 10 minutes and then was introduced into to a modified Novex® 10–20% Tricine gel (1.0 mm × 10 well) (Invitrogen, Carlsbad, CA). The gel was modified by using a scalpel to remove eight of the nine "teeth" at the top of the stacking gel. This produced two lanes from the original ten, one of width ≈7.0 cm and one remaining original well of width ≈0.8 cm. The cross-linked oligomer mixture was pipetted into the large lane. Molecular weight markers were pipetted into the small lane.

After SDS-PAGE, gels were washed in water three times for 5 min each time and then incubated in SimplyBlue™ SafeStain (Invitrogen, Carlsbad, CA) overnight on a ZD-9556 orbital shaker (Madell Technology, Ontario, CA) rotating at 60 rpm. The next morning, the gel was destained for 30 min and then incubated again with fresh SimplyBlue™ SafeStain for 2 hours. Afterwards, the gel was destained for 30 min in DDI water. Bands were excised using a scalpel blade (Fisher, Pittsburgh, PA) and placed in individual 1.5 mL microcentrifuge tubes.

***Modified "Cleveland Gel" System and Densitometry Analysis***

Gel pieces corresponding to each respective oligomer band excised from the preparative 10-20% acrylamide gel were re-electrophoresed in a second, larger gel using the Protean IIxi Cell Gel System (Bio-Rad, Hercules, CA), similar to the procedure of Cleveland *et al.* [16] that is used for separation of peptide fragments produced from gel slices treated with proteases *in situ* in polyacrylamide gel wells prior to electrophoresis. The gels were 1.5 mm in thickness, which accommodated the thickness of the excised slabs from the 1.0 mm Novex® 10–20% Tricine gel. The gels were made with an 18% T resolving polyacrylamide gel and a 4% T acrylamide

stacking gel, which provided the optimal separation of the extracted oligomers. A 20-well comb was inserted into the stacking gel during polymerization. Afterwards, the comb was removed and a scalpel was used to carefully excise the acrylamide gel between every other pair of wells to create nine larger wells (except for the first well, which was used for the MW marker (MWM)). Excised gel pieces containing the respective oligomers were boiled in 200 µL of 2× Novex Tricine SDS sample buffer (Invitrogen, Carlsbad, CA) for 10 min and then placed into individual lanes. An additional 30 µL of this same buffer then was added to each lane. Finally, Mark12™ Unstained Standard (Invitrogen, Carlsbad, CA) MWM were added to MWM well. To allow for better resolution and avoid overheating, the gel was run at 4°C at 50V for 5 hours and then the voltage was increased to 80V for 15-20 h. The gel was silver-stained using a Silver-Xpress silver staining kit (Invitrogen, Carlsbad, CA) and scanned with a Canon CanoScan 9950 flatbed scanner. Gel images were converted to 256 grayscale and analyzed using ImageJ 1.43r software ((http://imagej.nih.gov/ij/) to produce intensity profiles. To correct for overlapping peaks, the intensity profiles were imported into Magicplot Student v.2.0.1 (http://magicplot.com/), where non-linear curve fitting allowed overlapping peaks to be deconvoluted into individual peaks, assuming each peak was Gaussian in nature. The relative intensities were calculated based on the integration of the area under each fitted curve after baseline correction. Individual peak values were normalized to the total intensity within each lane. The data then were plotted using Kaleidagraph, v. 4.0.4 (Synergy Software, Reading, PA).

## RESULTS

### *Oligomer size distributions of wild type (WT) Aβ42 and its Tyr substituted variants*

We chemically synthesized Aβ42 variants with Tyr substituted at four different locations between the N- and C-termini: Asp1, Phe20, Ala30, and Ala42. To preclude intramolecular cross-linking occurring through the WT Tyr10 residue, we replaced this residue with Phe (Fig. 1). We then determined how the movement of Tyr across the Aβ42 peptide affected oligomerization, as monitored using PICUP, SDS-PAGE, and silver staining (Fig. 2). In the absence of cross-linking, Aβ42 and its four Tyr variants produced bands electrophoresing predominantly at monomer and trimer (filled white arrowheads). Less intense tetramer bands also were observed (open white arrowheads). These trimer and tetramer bands previously have been shown to be SDS-induced artifacts [9]. [Phe10, Tyr20]Aβ42 produced few SDS-stable oligomers. The predominant band was the monomer band, while only a faint trimer band (white arrowhead) was observed. The other four peptides all displayed tetramer bands, of which the tetramer band from [Phe10, Tyr42]Aβ42 was the most prominent (Fig. 2, open arrowheads).

Cross-linked WT Aβ42 produced eight bands corresponding to monomer through heptamer, with nodes at monomer and pentamer/hexamer (white arrowheads). [$Tyr^{1}$, $Phe^{10}$]Aβ42 produced a similar distribution, but with band mobilities shifted towards lower $M_r$ (relative molecular mass). These shifts also were observed in the non-cross-linked control. [$Phe^{10}$, $Tyr^{20}$]Aβ42 produced seven bands, corresponding to monomer through heptamer, with nodes at monomer and pentamer/hexamer (white arrowheads). The trimer band (open arrowhead) was fainter relative to those of the other oligomers. [$Phe^{10}$, $Tyr^{30}$]Aβ42 displayed a pattern of bands similar to WT Aβ42 (white arrowheads). [$Phe^{10}$, $Tyr^{42}$]Aβ42 behaved differently. The amount of dimer (white arrowhead) was lower relative to the other peptides and the amounts of heptamer,

octamer, and nonamer were greater. It appeared that Tyr substitutions closer to the C-terminus produced larger amounts of higher-order[1] oligomers.

***Stability of cross-linked oligomers***

To determine whether cross-linked Aβ42 oligomers were covalently associated, we performed PICUP reactions and fractionated the resulting products by SDS-PAGE. We excised bands identified by Coomassie Blue staining and then re-electrophoresed their component peptides by placing the gel pieces in wells of a second SDS gel. We predicted that covalently associated oligomers should produce a size-dependent "ladder" of bands corresponding to their initial $M_r$ values. Non-covalently associated oligomers, or oligomers that were not cross-linked completely, would produce multiple bands migrating at or below their initial observed $M_r$ values.

We made four observations in experiments using WT Aβ42 (Fig. 3a): (1) an order-dependent ladder of bands; (2) cross-linked oligomers of order 2-7 were unstable; (3) unstable oligomers produced lower order species varying in size from 1-6 (as predicted); and (4) bands of $M_r$ higher than the $M_r$ values of the originally isolated bands were observed. We quantified band intensities and then normalized these intensities for each lane (Fig. 3b; Table S1). These data showed that the most intense band in each lane corresponded to the $M_r$ of the band excised from the first SDS gel. The purest oligomer was dimer (67%). The least pure oligomer was tetramer (28%). In addition, relative to oligomers of order 2-5, purified hexamers and heptamers appeared more stable.

We next performed identical experiments using the four Tyr variants, [$Tyr^1$, $Phe^{10}$]Aβ42 (Fig. S1, Table S2), [$Phe^{10}$, $Tyr^{20}$]Aβ42 (Fig. S2, Table S3), [$Phe^{10}$, $Tyr^{30}$]Aβ42 (Fig. S3, Table S4), and [$Phe^{10}$, $Tyr^{42}$]Aβ42 (Fig. 4, Table S5). We observed behavior similar to that of wild type

[1] "Order" refers to the number of Aβ monomers comprising any assembly.

Aβ42 for the first three peptides (summarized in Table 1). In contrast, the [Phe$^{10}$, Tyr$^{42}$]Aβ42 peptide was exceptionally stable (cf. Figs. 3 and 4; Tables S1 and S5). The lowest purity observed was 81% (trimer), compared with 43% for the WT Aβ42. Similarly, the least stable WT Aβ42 oligomer, tetramer, was 28% pure, whereas the equivalent oligomer produced by [Phe$^{10}$, Tyr$^{42}$]Aβ42 was 75% pure. As suggested earlier, the higher-order oligomers were most stable. Pentamers, hexamers, and heptamers were all >90% pure. In some experiments, octamers and higher order oligomers also were observed in relatively pure form.

***Are "stable" Aβ42 oligomers really stable?***

Our prior experiments showed that replacing Ala42 with Tyr produced a peptide that produced cross-linked oligomers of exceptional stability. Nevertheless, we sought to subject these ostensibly stable oligomers to an additional denaturation/dissociation procedure to convince ourselves of their stability. To do so, we re-electrophoresed purified oligomers a second time (a total of three SDS gels). We performed identical experiments with WT Aβ42 so that we could compare the stabilities of the oligomers formed by each peptide. It is clear from inspection (cf. Figs. S4 and S5) that the [Phe$^{10}$, Tyr$^{42}$]Aβ42 peptide produced exceptionally stable oligomers. The purity of each oligomer was significantly greater than the corresponding oligomer formed by wild type Aβ42, with the exception of trimer (87% for [Phe$^{10}$, Tyr$^{42}$]Aβ42 versus 90% for wild type Aβ42) (Tables S6 and S7). Lower- and higher-order species were observed with wild type Aβ42, suggesting some instability of the purified oligomers (Fig. S4). In contrast, only faint dimer and trimer bands were observed in the tetramer and pentamer lanes with [Phe$^{10}$, Tyr$^{42}$]Aβ42 oligomers (Fig. S5).

## DISCUSSION

Formation of toxic Aβ42 oligomers is thought to be a seminal neuropathogenetic process in AD [17, 18]. If so, then design of oligomer-specific therapeutic agents requires the determination of structure–activity relationships (SAR) among the different types of oligomers. Unfortunately, the metastability and polydispersity of oligomer preparations has complicated this determination. The experiments conducted in this study demonstrate that positioning of a single Tyr residue at position 42 within Aβ42 allows the production and isolation of highly stable, pure populations of Aβ42 oligomers following photochemical cross-linking using the technique of PICUP.

Previous studies have shown that such PICUP is capable of revealing the distribution of Aβ oligomers present in an equilibrium state in which rapid association and dissociation reactions occur. These distributions were not stochastic, i.e., they did not represent distributions created by diffusion-limited monomer collisions [19]. This question was addressed experimentally and theoretically [20]. Briefly, the PICUP-generated oligomer distributions of two amyloidogenic (Aβ and human calcitonin (CT)) and two non-amyloidogenic (Human pituitary adenylate cyclase-activating polypeptide (PACAP) and human growth hormone-releasing factor (GRF)) peptides, all of similar molecular weight, were compared. We reasoned that amyloidogenic peptides, which are known to self-associate rapidly, should produce oligomer distributions reflective of the pre-existence of oligomers prior to execution of the cross-linking chemistry. In contrast, the non-amyloidogenic peptides would be expected to produce oligomer distributions reflective of oligomerization caused almost solely by diffusion-limited monomer collisions. These latter distributions would look like simple ladders, containing one node of intensity dependent on diffusion rates and peptide concentration. The former distributions would be distinct from those of the latter, and could contain multiple nodes. This was what we observed [9, 20]. We also modeled

the distributions mathematically by parameterizing a simple diffusion limited collisional oligomerization model with peptide concentration and chemical reactivity (efficiency). These distributions (see Fig. 6 in [20]) were contrasted with that obtained for Aβ40, revealing that the latter distribution was distinct, and therefore was not explainable by diffusion limited collisions of the monomer. The distributions also did not represent distributions obtained by partial cross-linking of much larger oligomers, as such oligomers were not found to exist [20]. Instead, the distributions comprised predominately oligomers of order 2-7 that pre-existed in solution. The data thus supported the conclusion that the PICUP chemistry produced accurate insights into the oligomer distribution.

Data supporting the relevance of cross-linked species to analyses of biophysical and neurotoxic properties of oligomers also has come from the salmon calcitonin amyloid system [21, 22]. Salmon calcitonin (sCT), like Aβ, appears to be intrinsically disordered, but capable of forming oligomers and α-helix-containing assembly intermediates. The α-helical state is relatively stable, which may explain why sCT fibril formation is a slow process. However, this fact has provided an opportunity to compare the oligomerization distributions of PICUP-cross-linked and non-cross-linked (native) sCT using SDS-PAGE [21]. The two distributions are highly similar, comprising predominately dimers and trimers, but each of these species is enriched after cross-linking. These data support the conclusion that cross-linking does not substantially alter the oligomerization or electrophoretic properties of the peptide, but simply stabilizes the oligomers against dissociation. The implication is that structure-activity relationships established in neurotoxicity experiments with cross-linked sCT are likely to reflect the same SAR established with non-cross-linked material. Induction suggests that cross-linked Aβ oligomers thus would

behave similarly to their non-cross-linked structural homologues, although this cannot formally be proven with current techniques.

Our experiments suggest, on average, that the stability of cross-linked oligomers increases as the Tyr is moved from the N-terminus to the C-terminus. This was especially true for oligomers of order greater than trimer, for which the purity of [Phe$^{10}$, Tyr$^{42}$]Aβ42 tetramer through heptamer was 75-92%, a range significantly higher than for the other peptides (e.g., [Tyr$^{1}$, Phe$^{10}$]Aβ42 had a range of 29-74%). The replacement of Ala42 with Tyr increases the hydrophobicity of the Aβ42 C-terminus, an effect that has been shown to facilitate formation of higher-order oligomers ($n>7$) [19]. This substitution also would be expected to stabilize a C-terminal turn in Aβ42 that is critical for oligomer stability [23]. In fact, we previously showed that Tyr substitution at residue 30 or 42 significantly diminishes its intrinsic fluorescence relative to substitution at positions 1, 10, or 20, a result suggesting stabilization or shielding of the Tyr [24]. Measurement of solvent accessible surface areas using molecular dynamics simulations are consistent with Tyr shielding at the C-terminus [25]. These studies also revealed that Aβ42 oligomer formation was predominantly driven by intermolecular interactions among the C-terminal regions. The stabilization within the C-terminus may play an important role in the oligomerization process and explain the rapid evolution of later assembly states such as protofibrils and fibrils. This suggests a simple mechanism by which the Tyr42 substitution leads to stably cross-linked oligomers—it maintains the Aβ42 monomers comprising the various oligomers in conformations amenable to rapid intermolecular cross-linking. In the absence of such structural stabilization, rapid conformational fluctuations in Aβ preclude the Tyr:Tyr interactions necessary for cross-linking during the short time span of the reaction (≈1 s). It is

interesting in this regard that recent studies of oligomers have used increased irradiation times (7-10 s) to perform the PICUP chemistry [26, 27].

We note that [Tyr$^{1}$, Phe$^{10}$]Aβ42 formed the least stable oligomers. It may be relevant in this regard that this peptide displayed a distinct oligomerization pattern relative to the other four peptides. All [Tyr$^{1}$, Phe$^{10}$]Aβ42 oligomer bands displayed lower $M_r$ values and the intensities of the pentamer and hexamer bands were relatively low. The anomalous migration of [Tyr$^{1}$, Phe$^{10}$]Aβ42 oligomers may be due to oligomer compaction [13], which could decrease cross-linking efficiency by stabilizing Tyr1 in a conformer that was less able to interact intermolecularly with other Aβ monomers. This phenomenon would be the mirror image of that operating in the [Phe$^{10}$, Tyr$^{42}$]Aβ42 system, in which C-terminal collapse contributed to stabilization of a conformer that could cross-link efficiently [25].

Intrinsic to our discussion of primary structure and oligomer stability (cross-linking efficiency) is the conformational space of each peptide system, i.e., what is the occupation frequency of each volume of that space? In simple terms, for how long does each of the many possible monomer and higher-order conformers exist? The answer to this question is related directly to the energies of formation of each conformer, which directly yield the probability that the particular conformer exists. For Aβ40 and Aβ42, we have addressed this question computationally [28], and from the probabilities thus obtained, we have been able to construct surfaces that allow direct visualization of the conformational spaces of each peptide. However, this question also can be addressed in the opposite manner, namely by starting with oligomer occurrence frequencies and then constructing models of each conformer. The matrices of nominal oligomer order versus oligomer frequency (Tables S1-S5) provide us the means to do so, as illustrated in Fig. 5.

The results of this analysis suggest that the formation of oligomers of order ≤7 occurs predominately through association of dimers and trimers (Fig. 5), as opposed to actin-type iterative monomer addition [29, 30]. This oligomerization mechanism explains the proclivity of Aβ42 to form paranuclei (pentamers and hexamers). Our suggestions are consistent with results of ion mobility spectrometry studies of Aβ oligomerization—which reveal oligomer distributions without the necessity for chemical cross-linking—that show that Aβ42 readily forms dimers, tetramers, hexamers, and dodecamers [31, 32]. Formation of tetramers and hexamers appears to occur by association of dimers, as opposed to dimer and monomer association. Of course, production of odd numbered oligomer units must require addition of monomers. Further studies will be necessary to determine the veracity of these suggestions.

## ACKNOWLEDGMENTS

We thank Margaret Condron for synthesizing and purifying the peptides used in this study.

## SUPPORTING INFORMATION AVAILABLE

Oligomer stability of [Tyr$^{1}$, Phe$^{10}$]Aβ42, [Phe$^{10}$, Tyr$^{20}$]Aβ42, [Phe$^{10}$, Tyr$^{30}$]Aβ42 are shown in Figures S1-S3. Stability of WT Aβ42 and [Phe10, Tyr42]Aβ42 oligomers after two consecutive Cleveland gel procedures are presented in Figures S4 and S5, respectively. Occurrence frequencies of oligomers of specific order produced from WT Aβ42 and its four singly substituted Tyr variants are presented in Tables S1-S5. Occurrence frequencies of WT and [Phe$^{10}$, Tyr$^{42}$]Aβ42 oligomers of specific order, analyzed following two consecutive Cleveland gels, are presented in Tables S6 and S7, respectively. This supporting material may be accessed free of charge online at http://pubs.acs.org.

**Table 1.** Oligomer stability of cross-linked WT Aβ42 and Aβ42 Tyr variants after Cleveland gel isolation. Values are percentage ± S.D.

| | Oligomer Order | | | | | | | |
|---|---|---|---|---|---|---|---|---|
| **Peptide** | **1** | **2** | **3** | **4** | **5** | **6** | **7** | **8** |
| **WT Aβ42** | 79 ± 5 | 67 ± 3 | 43 ± 1 | 28 ± 2 | 42 ± 3 | 52 ± 4 | 51 ± 4 | N/A |
| **[Y1,F10]Aβ42** | 93 ± 1 | 74 ± 3 | 36 ± 8 | 28 ± 5 | 43 ± 6 | 36 ± 1 | 52 ± 8 | N/A |
| **[F10,Y20]Aβ42** | 74 ± 3 | 64 ± 5 | 34 ± 6 | 41 ± 2 | 50 ± 2 | 63 ± 2 | 60 ± 2 | N/A |
| **[F10,Y30]Aβ42** | 79 ± 2 | 75 ± 7 | 46 ± 5 | 51 ± 4 | 71 ± 3 | 77 ± 3 | 76 ± 2 | N/A |
| **[F10,Y42]Aβ42** | 72 ± 2 | 82 ± 1 | 81 ± 2 | 75 ± 3 | 90 ± 1 | 92 ± 2 | 92 ± 1 | N/A |

**Table 2.** Oligomer stability of cross-linked WT Aβ42 and [Phe$^{10}$, Tyr$^{42}$]Aβ42 after two consecutive Cleveland gel isolations. Values are percentage ± S.D.

| | Oligomer Order | | | | | | | |
|---|---|---|---|---|---|---|---|---|
| **Peptide** | **1** | **2** | **3** | **4** | **5** | **6** | **7** | **8** |
| **WT Aβ42** | 96 ± 2 | 90 ± 2 | 90 ± 2 | 61 ± 5 | 59 ± 5 | 57 ± 4 | 64 ± 5 | 83 ± 2 |
| **[F10,Y42]Aβ42** | 96 ± 0.7 | 96 ± 1.4 | 87 ± 0.4 | 83 ± 3 | 91 ± 2.3 | 92 ± 1.3 | 92 ± 3 | N/A |

## FIGURE LEGENDS

**Fig. 1. Primary structures of Aβ42 peptides.** A Phe residue was substituted for Tyr10 in all peptides except WT. Amino acid differences between the WT sequence and those of the other four peptides are highlighted in red.

**Fig. 2. Oligomer size distributions of WT Aβ42 and its Tyr substituted variants.** PICUP, SDS-PAGE, and silver staining were used to determine oligomer size distributions. Eight µL of 40 µM peptide was loaded into each well, corresponding to 1.44 µg for the Aβ42 lanes and 1.47 µg for the [Phe10, Tyr42]Aβ42 lanes. Abbreviations are: MWM, molecular weight marker; $M_r$, relative molecular mass (Da); $Y^{\#}$, position of the Tyr in each respective peptide. $Y^{10}$ signifies wild type Aβ. Peptides were prepared and immediately electrophoresed ("non-cross-linked") or they were prepared, immediately cross-linked, and then electrophoresed ("cross-linked"). Arrowheads refer to specific bands (see text). Trimer and tetramer bands in the lanes of un-cross-linked are SDS-induced artifacts [9]. The starting material is aggregate-free.

**Fig. 3. WT Aβ42 oligomer stability.** Aβ42 was cross-linked and then electrophoresed in an SDS gel (see Methods). (a) Coomassie-stained oligomer bands were excised, re-electrophoresed, and the resulting bands visualized by silver staining. Each lane number represents the expected oligomer order. (b) Image J and MagicPlot software were used to determine the occurrence frequencies (%) of oligomers of each order. Data are representative of at least three independent experiments.

**Fig. 4. [Phe$^{10}$, Tyr$^{42}$]Aβ42 oligomer stability.** [Phe$^{10}$, Tyr$^{42}$]Aβ42 was cross-linked and then electrophoresed in an SDS gel (see Methods). (a) Coomassie-stained oligomer bands were excised, re-electrophoresed, and the resulting bands visualized by silver staining. Each lane number represents the expected oligomer order. (b) Image J and MagicPlot software were used to determine the occurrence frequencies (%) of oligomers of each order. Data are representative of at least three independent experiments.

**Fig. 5. Model of Aβ42 oligomerization.** The association and dissociation patterns observed for oligomer orders 2-7 (Figs. 2-4 and S1-S4), along with the occurrence frequencies for each oligomer (Tables S1-S5), were used to produce a model of oligomer formation. Simple monomer addition models, akin to actin polymerization [30], do not appear to explain these data. Instead, key roles are played by monomers, dimers, and trimers, which appear to act as building blocks for higher-order oligomers.

## REFERENCES

[1] Haass, C., and Selkoe, D. J. (2007) Soluble protein oligomers in neurodegeneration: lessons from the Alzheimer's amyloid β-peptide., *Nat Rev Mol Cell Biol 8*, 101-112.

[2] Dodart, J. C., Meziane, H., Mathis, C., Bales, K. R., Paul, S. M., and Ungerer, A. (1999) Behavioral disturbances in transgenic mice overexpressing the V717F β-amyloid precursor protein, *Behav Neurosci 113*, 982-990.

[3] Hsia, A. Y., Masliah, E., McConlogue, L., Yu, G. Q., Tatsuno, G., Hu, K., Kholodenko, D., Malenka, R. C., Nicoll, R. A., and Mucke, L. (1999) Plaque-independent disruption of neural circuits in Alzheimer's disease mouse models, *Proc Natl Acad Sci U S A 96*, 3228-3233.

[4] Moechars, D., Dewachter, I., Lorent, K., Reverse, D., Baekelandt, V., Naidu, A., Tesseur, I., Spittaels, K., Haute, C. V., Checler, F., Godaux, E., Cordell, B., and Van Leuven, F. (1999) Early phenotypic changes in transgenic mice that overexpress different mutants of amyloid precursor protein in brain, *J Biol Chem 274*, 6483-6492.

[5] Moechars, D., Lorent, K., and Van Leuven, F. (1999) Premature death in transgenic mice that overexpress a mutant amyloid precursor protein is preceded by severe neurodegeneration and apoptosis, *Neuroscience 91*, 819-830.

[6] Kumar-Singh, S., Dewachter, I., Moechars, D., Lubke, U., De Jonghe, C., Ceuterick, C., Checler, F., Naidu, A., Cordell, B., Cras, P., Van Broeckhoven, C., and Van Leuven, F. (2000) Behavioral disturbances without amyloid deposits in mice overexpressing human amyloid precursor protein with Flemish (A692G) or Dutch (E693Q) mutation, *Neurobiol Dis 7*, 9-22.

[7] Mucke, L., Masliah, E., Yu, G. Q., Mallory, M., Rockenstein, E. M., Tatsuno, G., Hu, K., Kholodenko, D., Johnson-Wood, K., and McConlogue, L. (2000) High-level neuronal expression of $A\beta_{1-42}$ in wild-type human amyloid protein precursor transgenic mice: Synaptotoxicity without plaque formation, *J Neurosci 20*, 4050-4058.

[8] Fancy, D. A., and Kodadek, T. (1999) Chemistry for the analysis of protein–protein interactions: Rapid and efficient cross-linking triggered by long wavelength light, *Proc Natl Acad Sci U S A 96*, 6020-6024.

[9] Bitan, G., Kirkitadze, M. D., Lomakin, A., Vollers, S. S., Benedek, G. B., and Teplow, D. B. (2003) Amyloid β-protein (Aβ) assembly: Aβ40 and Aβ42 oligomerize through distinct pathways, *Proc Natl Acad Sci U S A 100*, 330-335.

[10] Ono, K., Condron, M. M., and Teplow, D. B. (2009) Structure-neurotoxicity relationships of amyloid β-protein oligomers, *Proc Natl Acad Sci U S A 106*, 14745-14750.

[11] Roychaudhuri, R., Yang, M., Hoshi, M. M., and Teplow, D. B. (2009) Amyloid β-protein assembly and Alzheimer disease, *J Biol Chem 284*, 4749-4753.

[12] Lazo, N. D., Grant, M. A., Condron, M. C., Rigby, A. C., and Teplow, D. B. (2005) On the nucleation of amyloid β-protein monomer folding, *Protein Sci 14*, 1581-1596.

[13] Maji, S. K., Ogorzalek Loo, R. R., Inayathullah, M., Spring, S. M., Vollers, S. S., Condron, M. M., Bitan, G., Loo, J. A., and Teplow, D. B. (2009) Amino acid position-specific contributions to amyloid β-protein oligomerization, *J Biol Chem 284*, 23580-23591.

[14] Walsh, D. M., Hartley, D. M., Kusumoto, Y., Fezoui, Y., Condron, M. M., Lomakin, A., Benedek, G. B., Selkoe, D. J., and Teplow, D. B. (1999) Amyloid β-protein fibrillogenesis. Structure and biological activity of protofibrillar intermediates, *J Biol Chem 274*, 25945-25952.

[15] Bitan, G., and Teplow, D. B. (2004) Rapid photochemical cross-linking--A new tool for studies of metastable, amyloidogenic protein assemblies, *Acc Chem Res 37*, 357-364.

[16] Cleveland, D. W., Fischer, S. G., Kirschner, M. W., and Laemmli, U. K. (1977) Peptide mapping by limited proteolysis in sodium dodecyl sulfate and analysis by gel electrophoresis, *J Biol Chem 252*, 1102-1106.

[17] Kirkitadze, M. D., Bitan, G., and Teplow, D. B. (2002) Paradigm shifts in Alzheimer's disease and other neurodegenerative disorders: The emerging role of oligomeric assemblies, *J Neurosci Res 69*, 567-577.

[18] Klein, W. E. (2006) Cytotoxic intermediates in the fibrillation pathway: Aβ oligomers in Alzheimer's disease as a case study, In *Part A: Protein Misfolding, Aggregation, and Conformational Diseases* (Uversky, V. N., and Fink, A. L., Eds.), pp 61-75, Springer, New York.

[19] Bitan, G., Vollers, S. S., and Teplow, D. B. (2003) Elucidation of primary structure elements controlling early amyloid β-protein oligomerization, *J Biol Chem 278*, 34882-34889.

[20] Bitan, G., Lomakin, A., and Teplow, D. B. (2001) Amyloid β-protein oligomerization: prenucleation interactions revealed by photo-induced cross-linking of unmodified proteins, *J Biol Chem 276*, 35176-35184.

[21] Diociaiuti, M., Macchia, G., Paradisi, S., Frank, C., Camerini, S., Chistolini, P., Gaudiano, M. C., Petrucci, T. C., and Malchiodi-Albedi, F. (2014) Native metastable prefibrillar oligomers are the most neurotoxic species among amyloid aggregates, *Biochim Biophys Acta 1842*, 1622-1629.

[22] Meyer, J. P., Pelton, J. T., Hoflack, J., and Saudek, V. (1991) Solution structure of salmon calcitonin, *Biopolymers 31*, 233-241.

[23] Roychaudhuri, R., Yang, M., Deshpande, A., Cole, G. M., Frautschy, S., Lomakin, A., Benedek, G. B., and Teplow, D. B. (2013) C-terminal turn stability determines assembly differences between Aβ40 and Aβ42, *J Mol Biol 425*, 292-308.

[24] Maji, S. K., Amsden, J. J., Rothschild, K. J., Condron, M. M., and Teplow, D. B. (2005) Conformational dynamics of amyloid β-protein assembly probed using intrinsic fluorescence, *Biochemistry 44*, 13365-13376.

[25] Urbanc, B., Betnel, M., Cruz, L., Bitan, G., and Teplow, D. B. (2010) Elucidation of amyloid β-protein oligomerization mechanisms: discrete molecular dynamics study, *J Am Chem Soc 132*, 4266-4280.

[26] Chen, W. T., Hong, C. J., Lin, Y. T., Chang, W. H., Huang, H. T., Liao, J. Y., Chang, Y. J., Hsieh, Y. F., Cheng, C. Y., Liu, H. C., Chen, Y. R., and Cheng, I. H. (2012) Amyloid-β (Aβ) D7H mutation increases oligomeric Aβ42 and alters properties of Aβ-zinc/copper assemblies, *PLoS One 7*, e35807.

[27] Sugiki, T., and Utsunomiya-Tate, N. (2013) Site-specific aspartic acid isomerization regulates self-assembly and neurotoxicity of amyloid-β, *Biochem Biophys Res Commun 441*, 493-498.

[28] Yang, M., and Teplow, D. B. (2008) Amyloid β-protein monomer folding: free-energy surfaces reveal alloform-specific differences, *J Mol Biol 384*, 450-464.

[29] Oosawa, F., Asakura, S., and Ooi, T. (1961) Physical Chemistry of Muscle Protein "Actin", *Progress of Theoretical Physics Supplement 17*, 14-34.

[30] Oosawa, F., and Kasai, M. (1962) A theory of linear and helical aggregations of macromolecules, *J Mol Biol 4*, 10-21.

[31] Murray, M. M., Bernstein, S. L., Nyugen, V., Condron, M. M., Teplow, D. B., and Bowers, M. T. (2009) Amyloid β-protein: Aβ40 inhibits Aβ42 oligomerization, *J Am Chem Soc 131*, 6316-6317.

[32] Bernstein, S. L., Dupuis, N. F., Lazo, N. D., Wyttenbach, T., Condron, M. M., Bitan, G., Teplow, D. B., Shea, J. E., Ruotolo, B. T., Robinson, C. V., and Bowers, M. T. (2009) Amyloid-β protein oligomerization and the importance of tetramers and dodecamers in the aetiology of Alzheimer's disease, *Nat Chem 1*, 326-331.

| | |
|---|---|
| [Phe$^{10}$, Tyr$^{01}$]Aβ42 | **Y**AEFRHDSG**F**$^{10}$EVHHQKLVFF$^{20}$AEDVGSNKGA$^{30}$IIGLMVGGVV$^{40}$IA |
| [Tyr$^{10}$]Aβ42 | DAEFRHDSG**Y**$^{10}$EVHHQKLVFF$^{20}$AEDVGSNKGA$^{30}$IIGLMVGGVV$^{40}$IA |
| [Phe$^{10}$, Tyr$^{20}$]Aβ42 | DAEFRHDSG**F**$^{10}$EVHHQKLVF**Y**$^{20}$AEDVGSNKGA$^{30}$IIGLMVGGVV$^{40}$IA |
| [Phe$^{10}$, Tyr$^{30}$]Aβ42 | DAEFRHDSG**F**$^{10}$EVHHQKLVFF$^{20}$AEDVGSNKG**Y**$^{30}$IIGLMVGGVV$^{40}$IA |
| [Phe$^{10}$, Tyr$^{42}$]Aβ42 | DAEFRHDSG**F**$^{10}$EVHHQKLVFF$^{20}$AEDVGSNKGA$^{30}$IIGLMVGGVV$^{40}$I**Y** |

**Fig. 1**

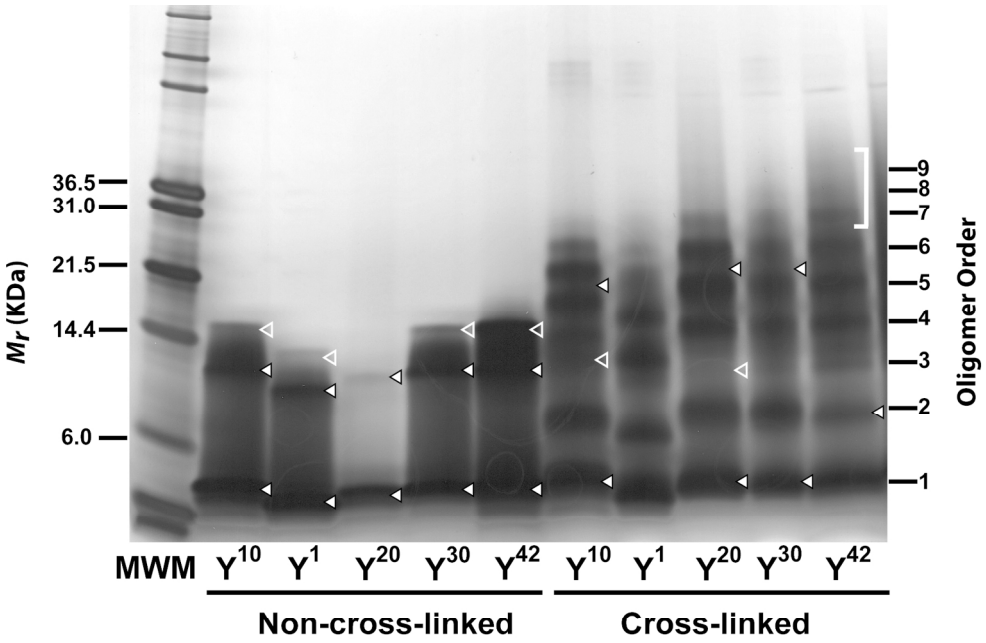


**Fig. 2**

157x112mm (300 x 300 DPI)

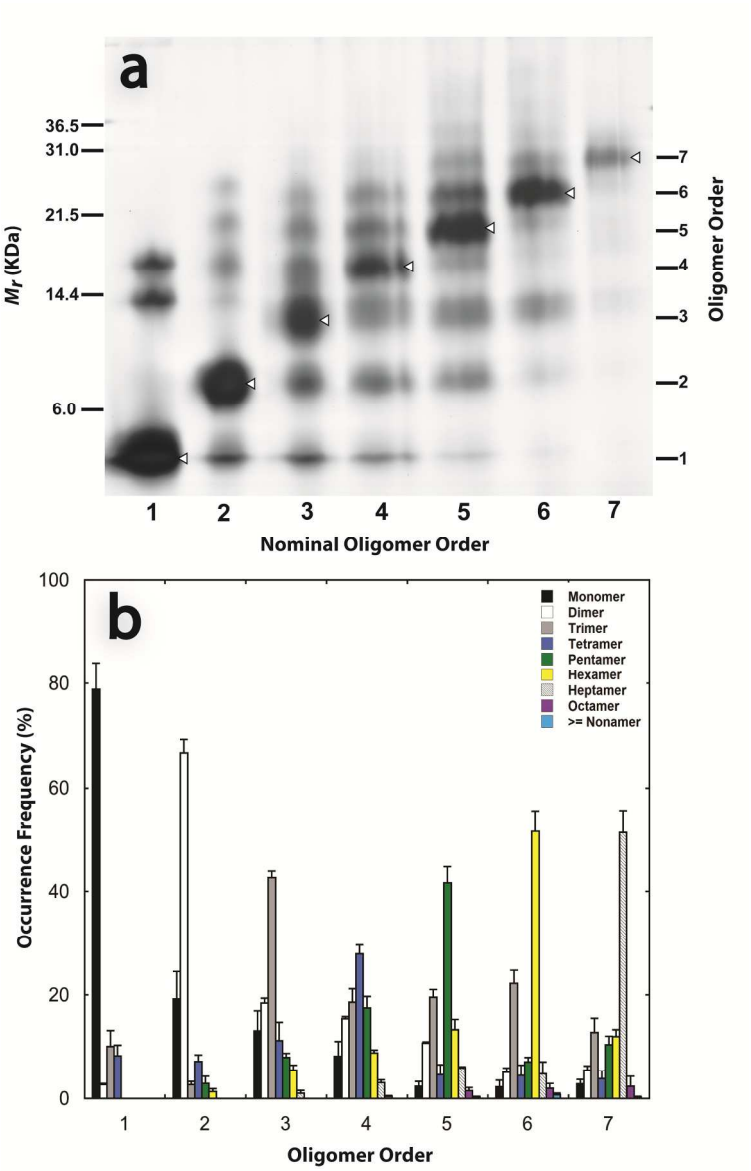


**Fig. 3**

151x243mm (300 x 300 DPI)

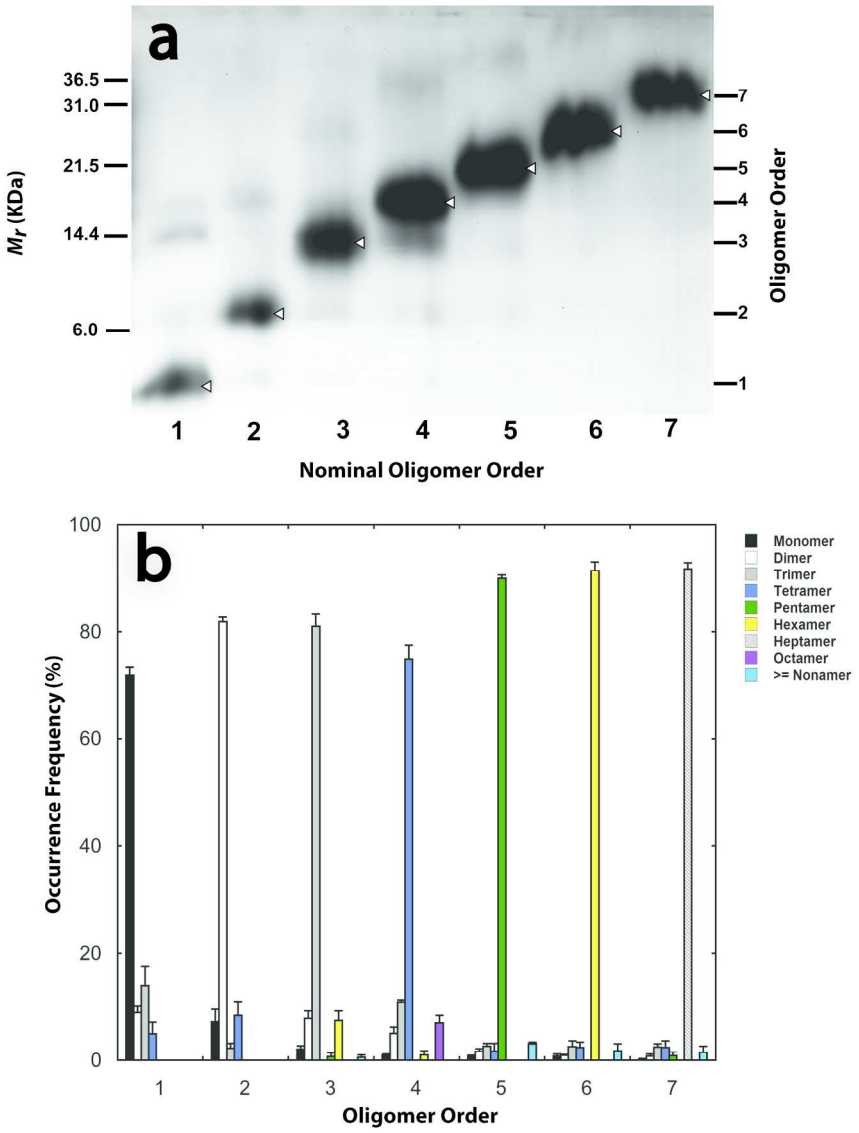


**Fig. 4**

162x228mm (300 x 300 DPI)

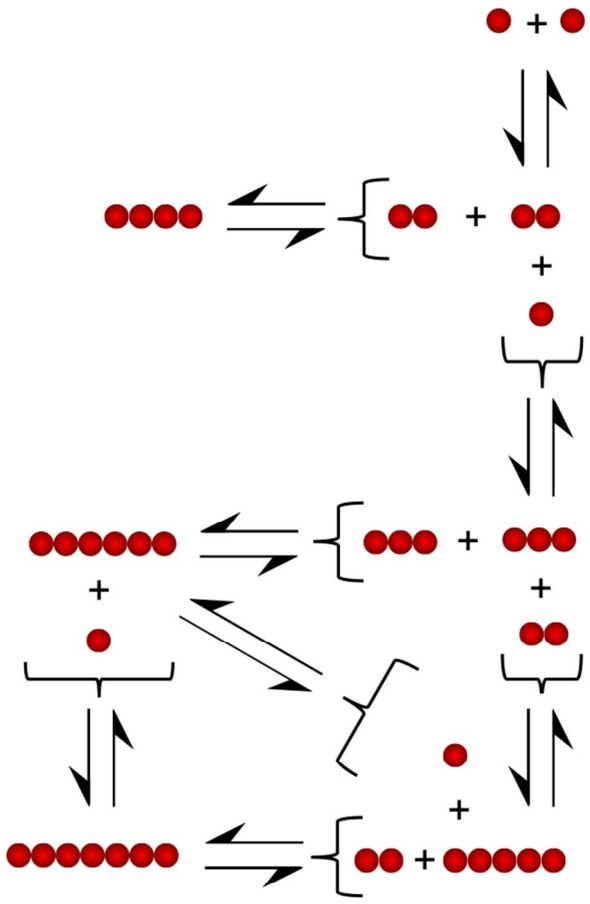

Fig. 5

299x430mm (72 x 72 DPI)

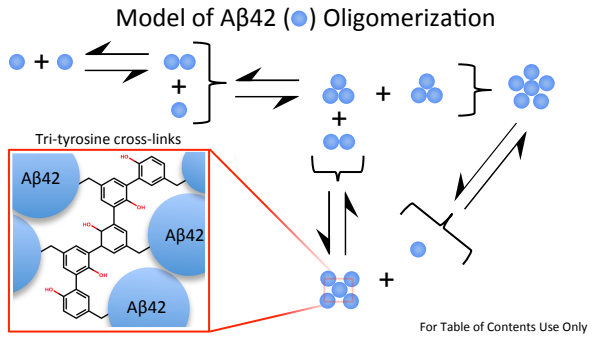
Model of Aβ42 (●) Oligomerization
Tri-tyrosine cross-links
Aβ42
Aβ42
Aβ42
For Table of Contents Use Only